ACTA CHEMICA SCANDINAVICA 26 (1972) 365–382

The Crystal Structure of Mo_8P_5 from Twin-crystal Data

TORSTEN JOHNSSON

Institute of Chemistry, University of Uppsala, Box 531, S-751 21 Uppsala 1, Sweden

The crystal structure of Mo_8P_5 has been determined by X-ray single-crystal methods. The symmetry is monoclinic (space group Pm) and the cell dimensions are $a = 9.399$ Å; $b = 3.209$ Å; $c = 6.537$ Å; $\beta = 109.59°$. The unit cell contains eight molybdenum and five phosphorus atoms situated in 1(a) or 1(b) positions. The structure can be described as a complex packing of triangular prisms of molybdenum atoms enclosing central phosphorus atoms.

Only twinned crystals have been obtained and the two types found are described. Some possible twin interface structures of minimum structural perturbation are discussed.

Some preliminary phase analytical results for the Mo–P system are presented.

At this Institute, a high temperature investigation of phosphides of transition metals is in progress, employing arc-melting as well as annealing treatments at well-defined temperatures. The latter technique is used in order to obtain equilibrium, and by using quenching to study phase relationships obtaining at high temperatures.[1,2] As a part of this project, the author has studied the region Mo_3P–MoP at temperatures from 900°C to about 1750°C.

The previously reported phases in this region are Mo_3P,[3] Mo_4P_3,[4] and MoP,[5] which all can be found below 1000°C.

EXPERIMENTAL AND PHASE ANALYTICAL RESULTS

Preparation and heat treatments. The phosphides were prepared by heating molybdenum powder (purity ~99.5 %) and red phosphorus (purity greater than 99 %) in evacuated and sealed silica tubes at temperatures between 900°C and 1100°C for about a week. In order to obtain the high-temperature modifications the samples were arc-melted in an atmosphere of purified argon. During this process there were moderate phosphorus losses. Annealings at high temperatures were performed in an induction furnace with an atmosphere of purified argon. The specimens were suspended within a cylindrical tantalum susceptor with a tantalum wire which was supported axially in the furnace. The samples could be quenched in cooled vacuum oil. The temperature was measured with an optical pyrometer, calibrated against a secondary standard tungsten ribbon lamp. The accuracy of the temperature measurements was estimated to be at least ±20°C.

During the annealings there were also some rather small phosphorus losses and these became larger for longer heating times. Thus a balance had to be struck between the desirability to heat the specimen for longer periods of time to obtain equilibrium, and the losses of phosphorus which this would entail.

Powder diffraction examination. Powder photographs were recorded using Guinier-Hägg focussing cameras with $CuK\alpha_1$ and $CrK\alpha_1$ radiation. Silicon ($a = 5.43054$ Å) was used as the internal calibration standard.

Preliminary phase analytical results. Three new phases have been found. All of them have been observed in arc-melted samples as well as in specimens which had been annealed after arc-melting. They all exist in the region $Mo_3P - Mo_4P_3$ and, on account of the phosphorus losses during the annealings, it has been difficult to determine the two-phase regions with Mo_4P_3 or other more phosphorus-rich phases.

A hexagonal phase denoted $Mo_{\sim 1.7}P$ has been observed and the cell parameters have been refined ($a = 16.6730 \pm 0.0010$ Å; $c = 3.3644 \pm 0.0004$ Å). It has been found to exist above about 1720°C and it has (in two-phase specimens) been observed only together with Mo_3P. $Mo_{\sim 1.7}P$ was also prepared (by arc-melting) and partially characterized crystallographically by Rundqvist and Nawapong.[6] The phase is also mentioned and its probable crystallographic relationships with other phases discussed by Lundström.[7]

Between about 1670°C and 1720°C there is a yet uncharacterized phase, which appears to have some crystallographic similarities with $Mo_{\sim 1.7}P$. It is found in "equilibrium" with Mo_3P and forms, probably within a very small temperature range, a two-phase region with Mo_8P_5.

In the temperature field 1580 – 1680°C a monoclinic phase, denoted Mo_8P_5, is stable. It is found in a two-phase region with Mo_3P, and with the uncharacterized phase mentioned above.

A more detailed analysis of the phase relationships in this part of the Mo – P system is in progress.

Single crystal examination of Mo_8P_5. Numerous attempts to obtain single crystals were made, both directly from arc-melted specimens as well as from samples which had been annealed after the arc-melting. X-Ray oscillation photographs showed that most of the individuals selected actually consisted of many smaller crystals. However, from the oscillation photographs (rotation about *b* or *c* axes) several of the individuals appeared to be single crystals. The Weissenberg photographs showed, however, that they invariably consisted of twins built up of at least two individuals. In relation to each other, the individuals were found to be orientated in two different ways. These orientions are described below.

The twinned crystal used for the structure determination was taken from a specimen which after arc-melting had been annealed at 1670°C for about 12 h. The twin measured about $0.02 \times 0.02 \times 0.05$ mm. As it was very irregular, and also on account of the twinning, no acceptable absorption correction could be performed. Diffraction patterns were recorded in an equi-inclination Weissenberg camera using Zr-filtred Mo*K*-radiation and Ni-filtred Cu*K*-radiation. The multiple film technique was used with (for Mo-radiation) iron foils interleaved with the films. The crystal was rotated about both the *b*-axis and the *c*-axis. From Mo-radiation the intensities, $I(hkl)$, for $k = 0 - 3$ and for $l = 0$, 1, and 4, respectively, were recorded and from the Cu-radiation for $k = 0$ and 1. For both the intensity data sets, the intensities of the layers with $k = 0$ and 1 were estimated visually using calibrated intensity scales.

Calculations. The unit cell dimensions of Mo_8P_5 were refined with a least-squares program. In the structure factor calculations the atomic scattering factors for molybdenum and phosphorus were obtained from Ref. 8, together with the real and imaginary parts of the dispersion factors. The structure was refined by the method of least-squares employing a weighting scheme according to Cruickshank *et al.*:[9] $w = 1/(a + |F_o| + c|F_o|^2)$ where the weighting constants *a* and *c* for the Mo-data (larger individual) were given the values 42.0 and 0.017, respectively. The calculations were performed on a CDC 3600 computer using the FORTRAN IV programmes listed in Table 1, Ref. 2.

INTERPRETATION OF THE WEISSENBERG PHOTOGRAPHS AND DESCRIPTION OF TWINNING

On all Weissenberg photographs double spots were observed. The films could be interpreted as arising from twinning in a crystal with monoclinic symmetry. The powder diffraction pattern could also be indexed on this basis, supporting the assumption of this symmetry.

At the best, there were twins with only two main individuals. In all cases there were also one or two additional smaller satellites. This was also the case for the "crystal" on which the structure determination was performed. However, it was possible to clearly identify and thereby disregard the reflexions from these small satellites.

Two different types of diffraction patterns (and accordingly two different twin orientations) were observed. They will henceforth be termed (type) A and B, respectively. The structure determination has been performed on the first type (A). The analysis of the B type twin was made using the information obtained from the A type.

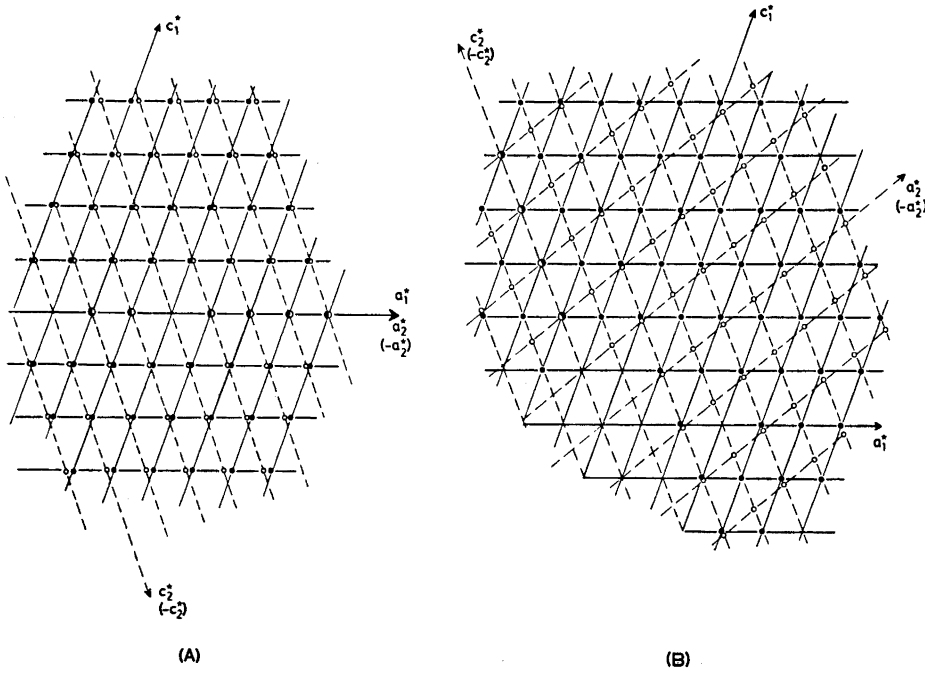

Fig. 1. h0l reciprocal lattice sections. Twin type A to the left and type B to the right. The reciprocal lattice of one individual is denoted with full circles and full lines, of the second individual with open circles and dashed lines. For type A, the lines parallel to the a^*-axis are common to both the individuals. Points common to both reciprocal lattices are marked as half-filled larger circles. Unobserved reflexions are omitted but no attempt has been made to indicate relative intensities.

Reciprocal lattice sections of the two types are given in Fig. 1. On both the types there is complete overlap (within experimental accuracy) along one "reciprocal axis", but along different "axes" for the two types.

Careful measurements of the films show, for both cases, that two reciprocal lattices orientated as in Fig. 1 can explain all the reflexions except some weaker ones, which from positions and intensity ratios could be assigned to the "extra" satellites mentioned above.

If the two twin individuals are of about the same size, which usually was found to be the case, it can be seen that type A will give two (false) symmetry lines, one along the a^*-axis and one 90° from there. This is one of the main features of films for this twin type.

First considering this type (A), it can be observed that when the directions of the reciprocal axes for the first individual (denoted "1" in Fig. 1 A) have been chosen, the directions of axes for the second can be chosen in two different ways (marked with and without parenthesis, respectively). The two alternatives cannot be distinguished from each other by means of the reciprocal lattice. However, they do correspond to different atomic arrangements.

The requirement that the three axes form a right-handed set leads to b_2^* being antiparallel to b_1^*.

The relation between the reflexions in one "pair" (one reflexion from each individual) is $h_2=h_1+l_1$ (or $h_2=-(h_1+l_1)$), $k_2=-k_1$ and $l_2=-l_1$ (or $l_2=l_1$).

For both the alternatives, Fig. 2 shows how the axes of the two individuals are oriented in relation to each other in the reciprocal and direct space. It can also be seen how a unit cell from each individual may be arranged.

The angle between the directions of the a-axes will be $2(\beta-90°)$ for this twin type, that is about 39° in this case.

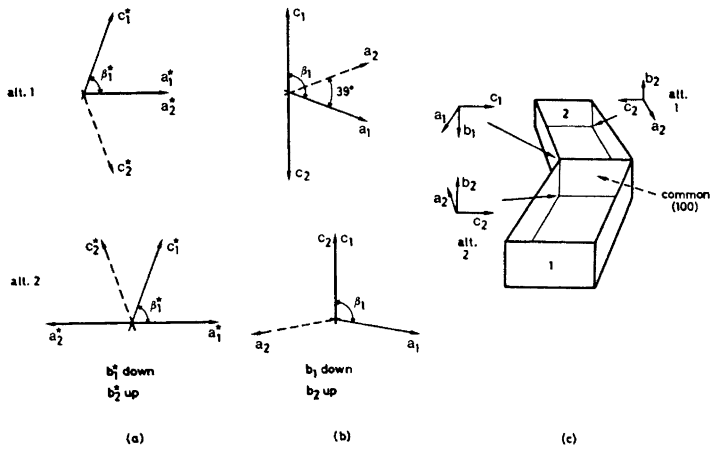

Fig. 2. Twin type A: The orientation relationships between the axes of the twinned (a) reciprocal and (b) direct lattices. The third figure (c) shows the relationship between the unit cells of the two individuals. (The diagram is only approximatively to scale.)

For alternative 1 the second individual can be made to coincide with the first one by a 180° rotation about the a^*-axis, that is about the normal to the (100) plane, which is then the twin plane. For alternative 2 coincidence can be obtained by a 180° rotation about the common c-axis and consequently [001] would be the twin axis. (Exchange of the operations between the two alternatives gives the other possible rotation for monoclinic systems given in Ref. 10, from which it is possible to see directly that there are two alternatives which cannot be distinguished by the lattice.) Another conceivable operation is given by reflexion across the (100) plane (for alt. 2 direct). However, this operation gives, in the present case, the same result as the rotation above, even as far as the atomic arrangement is concerned, depending on the fact that the structure is a "layer structure" (see below). The (100) plane is then the twin plane.

Photographs from a rotation about the c-axis confirmed the presumed twin orientation. Thus, on $hk0$ Weissenberg films all the reflexions are overlapped and as the two twin individuals are of about the same size, a pseudo-orthorhombic symmetry is apparent. On the $hk1$ films the spots have begun to separate, whereas on the $hk4$ films all the reflexions are separated, including those along the a^*-axis.

According to Friedel's classification [11] the crystals are twinned by pseudo-merohedry, rotation or reflexion twins. The obliquity [11,17] is about 19.6°.

Twins of this or similar sorts have been studied in detail, amongst others, by Herbstein [12–14] and by Grainger and McConnell.[15,16] Grainger has also given methods for interpreting Weissenberg photographs of pseudo-merohedral twins [17] and methods for the treatment of overlapped data.[18]

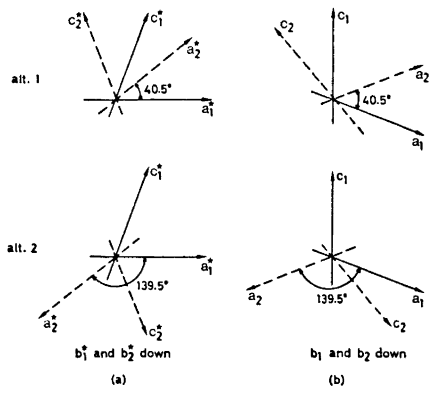

Fig. 3. Twin type B: The orientation relationships between the axes of the twinned (a) reciprocal and (b) direct lattices.

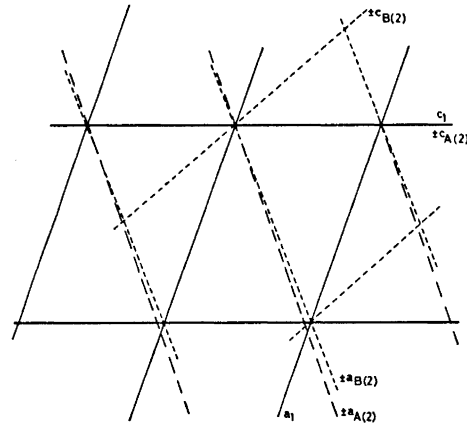

Fig. 4. Lattice projection on the (010) plane. Individual "1" (common to type A and B) is denoted: ———. Individual "2" for type A, A(2): – – – and for type B, B(2): - - - - -. Lines common to "1" and A(2): ———.

Whilst the twin of type A is of a rather well-known kind, the other type (B) is probably more unusual.

From the reciprocal lattice in Fig. 1 B it is possible, as in the previous case, to obtain two alternatives for the axes of individual 2. Fig. 3 shows the two possibilities in the reciprocal and direct space. The second individual can be made to coincide with the first one by turning 40.5° (or 139.5°) around the *b*-axis. This is not a permitted twin operation [10,11] and consequently twin type B will not be a "true twin".[11]

The angle between the *a*-axes of the two individuals (40.5°) corresponds (within experimental accuracy) to the angle between the *a*-axis and the direction of a face diagonal. The directions of the *b*-axes are common. Thus, "the common plane" will be ($\bar{1}01$) for "individual 1" and (001) for "individual 2". This can also be seen from the reciprocal lattice in Fig. 1 B.

It may be pointed out that the two twin types are connected in a certain way. Let "individual 1" be the starting point in both cases. If "individual 2" for the two alternatives in type A is rotated 180° about its *a*-axis the arrangement for "individual 2" in type B is *almost* obtained. (This rotation is a permitted twin operation.) Reflexion across (001) gives the same result (*cf.* the discussion of the layer structure above). However, it will not exactly correspond to the arrangement of the B-type, which can be seen from the different angles between the *a*-axes (39° and 40.5° for type A and B, respectively). This will be clear from Fig. 4, where "individual 1" is common for both types and the different "individuals 2" (A(2) and B(2)) are shown in relation to it.

DETERMINATION OF THE CRYSTAL STRUCTURE

Preliminary observations. As previously mentioned, it could be seen from the Weissenberg and oscillation photographs that the symmetry is monoclinic. The powder diffraction pattern could be indexed starting with the approximate unit cell dimensions obtained from a set of single crystal photographs. All the observed reflexions could be interpreted. Powder diffraction data are given in Table 1 and the cell dimensions with standard deviations in Table 3. The values in these tables are derived from photographs taken with Cr$K\alpha_1$ radiation. The diffraction pattern with Cu$K\alpha_1$ radiation gave results which were in full accordance with these data.

As no systematic extinctions were observed the possible space groups are $P2$, Pm, or $P2/m$. A comparison between the intensities of the layers $h0l$ and $h2l$ on the one hand and the layers $h1l$ and $h3l$ on the other showed striking similarities. This observation, together with the fact that the *b*-axis is very short, indicates that the atoms of the unit cell are confined to two planes perpendicular to the *b*-axis, with a spacing of $b/2$.

The composition of the compound remained somewhat uncertain, since it was not possible to prepare homogeneous single phase samples in sufficient amounts for ordinary chemical analysis. It was also hard to estimate the phosphorus losses during the heat treatments. However, a comparison of the unit cell volume with the cell volumes of Mo_3P, $Mo_{\sim 1.7}P$, and Mo_4P_3 suggested a cell content of 13 atoms, the probable composition thus being Mo_8P_5.

Table 1. Powder diffration data for Mo_8P_5. Guinier-Hägg camera with $CrK\alpha_1$ radiation. I_c on a relative scale with $I_c(\text{max.}) = 100$.

h	k	l	$\sin^2\theta \times 10^5$		I	
			obs	calc	obs	calc
1	0	0		1671		0.5
0	0	1	3456	3456	VVW	1.5
1	0	−1	3543	3515	VW	6.1
2	0	0		6686		1.2
1	0	1	6731	6739	VW	2.6
2	0	−1	6935	6918	VW	4.4
1	0	−2		12270		0.8
0	1	0	12725	12729	M	14.6
2	0	1[a]	13329	13365	ST	17.3
3	0	−1	13669	13663	W	8.4
0	0	2	13811	13822	VW	3.8
2	0	−2	14070	14061	VVW	3.0
1	1	0	14379	14400	VW	4.9
3	0	0		15043		0.1
0	1	1	16199	16184	M	9.6
1	1	−1	16250	16244	M	13.4
1	0	2	18709	18717	ST	51.1
3	0	−2	19188	19195	ST	67.6
2	1	0		19414		4.2
1	1	1	19459	19467	ST	100.0
2	1	−1	19631	19646	ST	93.5
3	0	1[b]	23371	23334	ST	28.9
4	0	−1	23741	23751	M	27.4
1	1	−2	25009	24999	M	39.3
2	1	1	26096	26093	ST	76.8
3	1	−1	26386	26392	ST	76.5
0	1	2	26546	26551	ST	78.9
4	0	0	26750	26743	ST	95.3
2	1	−2	26783	26790	ST	88.5
2	0	2	26965	26955	W	25.5
4	0	−2	27665	27671	W	21.5
3	1	0	27776	27771	ST	97.6
1	0	−3	27944	27937	ST	79.0
2	0	−3	28112	28116	W	39.3
0	0	3	31115	31101	VW	9.9
1	1	2	31450	31446	M	63.2
3	0	−3		31638		4.1
3	1	−2	31943	31923	M	60.7
3	1	1	36067	36062	W	20.4
4	1	−1	36469	36480	VW	19.0
4	0	1		36645		4.8
5	0	−1	37202	37183	VVW	11.3
1	0	3		37607		2.5
4	0	−3	38532	38502	VVW	3.1
3	0	2		38536		3.8
4	1	0	39486	39471	VW	7.3
5	0	−2		39491		2.6
2	1	2	39700	39684	W	23.1
4	1	−2	40414	40400	VW	20.1
1	1	−3	40659	40665	W	24.0
2	1	−3	40818	40844	VW	17.3
5	0	0	41751	41786	VW	13.7
0	1	3		43829		1.2
3	1	−3		44366		3.0
2	0	3	47427	47457	VW	11.7
5	0	−3	48729	48710	VW	27.6

[a] Overlapped by a line belonging to the calibration substance (Si).
[b] Overlapped by a line belonging to the phase Mo_3P.

*Single crystal diffraction with Cu*K-*radiation.* When examining twins by single crystal diffraction methods two somewhat different approaches are possible. One can try to obtain as many separated reflexions as possible, or try to work entirely with overlapped data. The first method requires the use of radiation with as long a wavelength as possible, and therefore diffraction data from the two layer lines (*h*0*l*) and (*h*1*l*) with Cu*K* radiation were recorded and the intensities estimated. The reflexions along the *a**-axis, which for this twin type (A) are overlapped, are the only ones which are *not* separated on these films.

If $(hkl)_1$ and $(hkl)_2$ are the indices for the same reflexion from twin individuals "1" and "2", respectively, then the ratio $I(hkl)_2/I(hkl)_1$ would be the same for all reflexions. The value of this ratio is determined by the volume ratio of the individuals. Because of the high absorption when using Cu-radiation the observed variation in this ratio is here very large. However, the mean value (1.2) was used to separate the overlapped reflexions along the *a**-axis. This is possible because these reflexions have identical indices for both individuals. By estimating the intensities from both the twin individuals and comparing, for different reflexions the ratio mentioned above, one obtains an additional check on the intensity estimation and on the correctness of the assumption of the twinning orientation. The material from the larger individual was used for further work.

In order to determine the structure the Patterson functions $P(U0W)$ and $P(U\frac{1}{2}W)$ were calculated. The Patterson sections were analyzed without introducing any assumption of centrosymmetry. Only simple super-position methods were used, and an arrangement of eight (onefold) molybdenum atoms was eventually found to explain the largest maxima in the Patterson maps satisfactorily. Probable positions of five phosphorus atoms could be derived from spatial considerations. With the atomic positions thus obtained the heights and positions of all the peaks in the Patterson maps could be explained. The space group is probably *Pm* with all the atoms in onefold positions, a symmetry which is very low for a compound of this sort.

Electron density calculations, initially with only the metal atoms, and subsequently with all the 13 atoms confirmed that the atomic positions determined from the Patterson analysis were approximately correct. These positions were improved by means of electron density maps, and a least-squares refinement was then started with the improved values.

The structure was refined using a full matrix least-squares program. 39 parameters were varied during the refinement, *viz.* 24 positional parameters (one metal atom was fixed in 0,0,0), 13 isotropic temperature factors, and two scale factors. 270 *h*0*l* and *h*1*l* reflexions were used. The final *R*-value ($R = \sum||F_o| - |F_c||/\sum|F_o|$) at this stage was about 0.18.

*Single crystal diffraction with Mo*K-*radiation.* In order to get further substantiation of the structure analysis described above, the intensity material from the layer lines (*h*0*l*) and (*h*1*l*) with Mo*K*-radiation was estimated. In comparison with the Cu-material there are more reflexions and less absorption but on the other hand more reflexions will be overlapped in the Mo-material.

For the same reasons as mentioned above, all the reflexions from both the individuals were estimated. The mean value of the ratio $I(hkl)_2/I(hkl)_1$ is here

Table 2. Observed and calculated structure factors (Mo-data). Reflexions not included in the last cycles of refinement are marked with an asterisk. The reflexions with higher indices on the festoons with $l=1$ and -1 could not be observed in the Cu-material and these overlapped reflexions in the Mo-material could not be separated with the method used here.

h	k	l	$\|F_o\|$	$\|F_c\|$	
1	0	0	-	3.7	
2	0	0	-	11.9	
3	0	0	-	6.0	
4	0	0	150.3	200.8	*
5	0	0	76.5	78.1	
6	0	0	41.5	34.8	
7	0	0	46.4	41.2	
8	0	0	45.5	38.2	
9	0	0	73.4	66.2	
10	0	0	97.1	86.7	
11	0	0	80.5	71.8	
12	0	0	41.0	30.3	
13	0	0	46.6	39.3	
14	0	0	72.1	81.6	
15	0	0	81.2	96.5	
16	0	0	46.9	48.8	
17	0	0	43.7	43.9	
18	0	0	37.5	44.2	
19	0	0	63.9	90.2	
1	0	-1	-	18.6	
2	0	-1	-	22.7	
3	0	-1	55.2	44.6	
4	0	-1	107.7	104.1	*
5	0	-1	62.5	72.3	
6	0	-1	50.0	47.2	
7	0	-1	65.1	77.8	
8	0	-1	73.5	89.8	
9	0	-1	56.2	59.0	
10	0	-1	54.1	61.1	
11	0	-1	68.0	64.3	
12	0	-1	-	66.0	
13	0	-1	-	39.9	
14	0	-1	-	27.6	
15	0	-1	-	39.5	
16	0	-1	-	28.7	
17	0	-1	-	10.1	
18	0	-1	-	17.7	
19	0	-1	-	18.6	
0	0	1	-	9.0	
1	0	1	-	17.3	
2	0	1	67.4	63.8	
3	0	1	103.0	106.6	*
4	0	1	44.1	47.1	
5	0	1	49.7	51.7	
6	0	1	67.7	93.6	
7	0	1	66.6	85.2	
8	0	1	57.6	56.3	
9	0	1	71.1	72.2	
10	0	1	60.4	61.8	
11	0	1	-	38.1	
12	0	1	-	52.0	
13	0	1	-	31.1	
14	0	1	-	32.0	
15	0	1	-	36.2	
16	0	1	-	47.2	
17	0	1	-	25.7	
18	0	1	-	53.9	
1	0	-2	-	13.0	
2	0	-2	33.4	27.0	
3	0	-2	126.6	150.1	*
4	0	-2	96.7	96.2	
5	0	-2	39.8	34.7	
6	0	-2	59.1	57.1	
7	0	-2	96.4	96.8	
8	0	-2	88.4	89.3	
9	0	-2	49.0	45.9	
10	0	-2	-	28.4	
11	0	-2	-	15.3	
12	0	-2	59.0	51.7	
13	0	-2	46.7	39.8	
14	0	-2	49.4	49.7	
15	0	-2	75.1	74.7	
16	0	-2	-	31.0	
17	0	-2	46.4	41.5	
18	0	-2	-	73.0	
19	0	-2	-	67.7	
0	0	2	32.9	30.4	
1	0	2	118.3	129.5	*
2	0	2	95.7	104.0	
3	0	2	51.1	41.6	
4	0	2	66.3	62.8	
5	0	2	66.9	65.6	
6	0	2	107.4	101.4	
7	0	2	66.5	55.9	
8	0	2	80.5	64.2	
9	0	2	-	12.0	
10	0	2	107.3	88.3	
11	0	2	55.1	43.2	
12	0	2	53.9	45.3	
13	0	2	44.3	37.7	
14	0	2	48.2	51.5	
15	0	2	49.7	41.0	
16	0	2	-	40.0	
17	0	2	-	52.6	
1	0	-3	128.6	185.2	*
2	0	-3	104.1	130.8	*
3	0	-3	44.2	43.5	
4	0	-3	39.0	37.8	
5	0	-3	100.1	102.4	
6	0	-3	117.1	134.1	
7	0	-3	25.7	20.6	
8	0	-3	90.6	84.2	
9	0	-3	56.0	51.9	
10	0	-3	89.8	77.8	
11	0	-3	65.6	57.9	
12	0	-3	108.6	113.7	
13	0	-3	55.0	43.9	
14	0	-3	43.9	35.9	
15	0	-3	39.9	39.3	
16	0	-3	89.9	96.2	
17	0	-3	-	15.5	
18	0	-3	-	19.5	
19	0	-3	-	53.9	
0	0	3	63.4	67.0	
1	0	3	37.6	34.2	
2	0	3	76.6	68.4	
3	0	3	144.1	168.9	*
4	0	3	29.0	22.7	
5	0	3	72.4	65.3	
6	0	3	40.8	38.1	
7	0	3	72.8	58.4	
8	0	3	44.8	38.2	
9	0	3	104.3	95.5	
10	0	3	-	23.2	
11	0	3	-	19.1	
12	0	3	51.3	47.1	
13	0	3	99.6	109.1	
14	0	3	-	8.7	
15	0	3	-	39.7	
16	0	3	-	47.5	
17	0	3	-	65.2	
1	0	-4	61.2	60.7	
2	0	-4	55.6	52.2	
3	0	-4	65.4	69.4	
4	0	-4	57.8	59.4	
5	0	-4	68.4	82.1	
6	0	-4	44.8	41.1	
7	0	-4	71.2	69.1	
8	0	-4	-	12.9	
9	0	-4	86.7	78.8	
10	0	-4	-	8.1	
11	0	-4	79.2	68.4	
12	0	-4	-	9.2	
13	0	-4	72.4	61.2	
14	0	-4	-	13.8	
15	0	-4	51.5	46.4	
16	0	-4	-	4.5	
17	0	-4	-	26.9	
18	0	-4	56.4	54.7	
19	0	-4	-	19.8	
0	0	4	51.6	52.5	
1	0	4	49.2	57.6	
2	0	4	37.4	32.0	
3	0	4	69.6	69.3	
4	0	4	-	6.3	
5	0	4	79.4	65.5	
6	0	4	34.9	31.8	
7	0	4	67.6	59.4	
8	0	4	43.8	35.5	
9	0	4	92.7	78.9	
10	0	4	-	13.7	
11	0	4	53.9	40.2	
12	0	4	67.5	63.6	
13	0	4	-	33.7	
14	0	4	-	6.2	
15	0	4	-	49.5	
16	0	4	-	52.6	
1	0	-5	46.8	46.0	
2	0	-5	41.0	43.9	
3	0	-5	59.2	73.6	
4	0	-5	86.5	103.1	
5	0	-5	87.1	101.0	
6	0	-5	60.1	57.4	
7	0	-5	30.8	30.0	
8	0	-5	-	17.9	
9	0	-5	88.0	88.0	
10	0	-5	81.3	69.6	
11	0	-5	66.3	54.3	
12	0	-5	63.7	50.8	
13	0	-5	-	38.5	
14	0	-5	44.4	37.8	
15	0	-5	94.7	98.1	
16	0	-5	59.0	57.7	
17	0	-5	55.4	42.8	
18	0	-5	-	17.2	
19	0	-5	-	96.7	
0	0	5	97.3	126.1	
1	0	5	73.2	93.4	
2	0	5	-	10.8	
3	0	5	-	18.0	
4	0	5	105.4	93.4	
5	0	5	116.7	119.4	
6	0	5	67.5	60.1	
7	0	5	52.8	42.1	
8	0	5	51.4	41.2	
9	0	5	90.0	64.5	
10	0	5	67.0	54.5	
11	0	5	-	13.5	
12	0	5	49.4	44.0	
13	0	5	-	49.9	
14	0	5	-	50.2	
15	0	5	-	47.9	
1	0	-6	33.1	30.1	
2	0	-6	-	18.1	
3	0	-6	100.4	120.1	
4	0	-6	29.2	30.9	
5	0	-6	31.4	30.0	
6	0	-6	66.6	62.3	
7	0	-6	103.7	111.5	
8	0	-6	60.4	58.8	
9	0	-6	74.1	55.6	
10	0	-6	84.8	77.9	
11	0	-6	74.2	68.8	
12	0	-6	50.8	48.4	
13	0	-6	45.1	41.9	
14	0	-6	67.8	70.4	
15	0	-6	-	35.0	
16	0	-6	-	38.6	
17	0	-6	-	29.0	
18	0	-6	-	45.5	
19	0	-6	-	34.1	
0	0	6	59.3	59.3	
1	0	6	80.7	86.5	
2	0	6	50.4	46.8	
3	0	6	-	24.3	
4	0	6	59.4	52.6	
5	0	6	48.1	45.7	
6	0	6	50.3	43.2	
7	0	6	-	15.2	
8	0	6	63.4	64.2	
9	0	6	63.2	63.3	
10	0	6	-	28.4	
11	0	6	-	45.5	
12	0	6	-	75.6	
13	0	6	-	71.1	
14	0	6	-	12.6	
1	0	-7	61.2	48.7	
2	0	-7	65.2	68.0	
3	0	-7	34.6	31.7	
4	0	-7	34.7	29.3	
5	0	-7	-	21.3	
6	0	-7	43.5	32.0	
7	0	-7	-	20.9	
8	0	-7	37.3	33.4	
9	0	-7	56.0	58.0	
10	0	-7	39.9	42.7	
11	0	-7	60.2	49.9	
12	0	-7	52.7	59.4	
13	0	-7	49.9	43.7	
14	0	-7	-	29.6	
15	0	-7	63.3	65.6	
16	0	-7	-	35.5	
17	0	-7	-	28.9	
18	0	-7	-	46.8	
19	0	-7	-	61.3	
0	0	7	62.5	63.5	
1	0	7	41.4	40.1	
2	0	7	85.4	81.9	
3	0	7	59.3	46.2	
4	0	7	66.3	54.6	
5	0	7	-	27.7	
6	0	7	73.4	70.1	
7	0	7	-	30.1	
8	0	7	47.5	42.6	
9	0	7	-	22.1	
10	0	7	-	31.8	
11	0	7	-	28.1	
12	0	7	-	16.9	
13	0	7	-	8.0	
1	0	-8	71.1	66.9	
2	0	-8	94.1	96.3	
3	0	-8	57.2	57.6	
4	0	-8	65.9	81.4	
5	0	-8	46.8	41.0	
6	0	-8	106.7	129.5	
7	0	-8	70.6	64.3	
8	0	-8	46.7	46.9	
9	0	-8	61.4	62.4	
10	0	-8	64.8	67.9	
11	0	-8	57.4	51.5	
12	0	-8	50.0	45.6	
13	0	-8	56.5	53.9	
14	0	-8	49.5	48.4	
15	0	-8	-	28.2	
16	0	-8	65.9	76.4	
17	0	-8	-	41.5	
18	0	-8	-	76.6	
19	0	-8	-	32.2	
0	0	8	59.6	69.5	
1	0	8	-	35.0	
2	0	8	-	21.0	
3	0	8	77.5	81.8	
4	0	8	70.1	66.1	
5	0	8	-	21.0	
6	0	8	74.5	78.3	
7	0	8	48.4	46.7	
8	0	8	67.1	77.3	
9	0	8	-	51.1	
10	0	8	-	92.1	
11	0	8	-	26.0	
1	0	-9	52.1	48.7	
2	0	-9	-	23.7	
3	0	-9	48.7	38.2	
4	0	-9	60.3	63.5	
5	0	-9	-	9.5	
6	0	-9	-	9.5	
7	0	-9	49.3	46.8	
8	0	-9	56.6	58.8	
9	0	-9	-	27.5	
10	0	-9	-	27.2	
11	0	-9	49.9	59.6	
12	0	-9	59.3	53.7	
13	0	-9	47.7	46.5	
14	0	-9	48.8	43.1	
15	0	-9	-	63.0	
16	0	-9	-	59.7	
17	0	-9	-	36.3	
18	0	-9	-	31.5	
0	0	9	63.0	63.3	
1	0	9	51.6	48.3	
2	0	9	52.8	36.0	
3	0	9	61.2	57.4	
4	0	9	-	34.5	
5	0	9	-	30.9	
6	0	9	-	39.0	
7	0	9	-	33.5	
8	0	9	-	35.0	
9	0	9	-	35.8	
10	0	9	-	36.1	
1	0	-10	-	14.2	
2	0	-10	-	34.8	
3	0	-10	-	32.9	
4	0	-10	44.8	40.2	
5	0	-10	-	26.4	
6	0	-10	52.4	54.5	
7	0	-10	-	21.7	
8	0	-10	45.6	47.3	
9	0	-10	46.2	47.3	
10	0	-10	70.3	74.2	
11	0	-10	-	9.1	
12	0	-10	64.1	76.3	
13	0	-10	-	29.8	
14	0	-10	-	63.0	
15	0	-10	-	17.8	
16	0	-10	-	45.1	
17	0	-10	-	35.5	
18	0	-10	-	31.4	
0	0	10	61.6	48.3	
1	0	10	62.6	65.3	
2	0	10	56.3	65.6	
3	0	10	59.9	44.3	
4	0	10	-	56.4	
5	0	10	-	61.8	
6	0	10	-	42.4	
7	0	10	-	47.8	
8	0	10	-	28.2	
1	0	-11	54.5	45.5	
2	0	-11	68.3	77.3	
3	0	-11	72.0	89.3	
4	0	-11	52.3	46.5	
5	0	-11	58.4	62.7	
6	0	-11	77.1	95.3	
7	0	-11	63.3	69.8	
8	0	-11	-	28.5	
9	0	-11	51.2	57.5	
10	0	-11	59.9	72.2	
11	0	-11	-	46.3	
12	0	-11	-	18.4	
13	0	-11	-	17.7	
14	0	-11	-	51.1	
15	0	-11	64.4	72.5	
16	0	-11	-	32.0	
17	0	-11	-	2.0	
0	0	11	69.6	59.5	
1	0	11	-	28.6	
2	0	11	-	49.3	
3	0	11	-	20.4	
4	0	11	-	46.3	
5	0	11	-	62.5	
6	0	11	-	42.2	
1	0	-12	-	45.6	
2	0	-12	-	14.5	
3	0	-12	-	31.9	
4	0	-12	-	20.9	
5	0	-12	-	19.7	
6	0	-12	-	20.9	
7	0	-12	-	22.6	
8	0	-12	-	15.2	
9	0	-12	-	29.3	
10	0	-12	-	33.6	
11	0	-12	-	56.0	
12	0	-12	-	34.2	
13	0	-12	-	67.4	
14	0	-12	-	31.3	
15	0	-12	-	67.8	
0	0	12	-	34.0	
1	0	12	-	49.3	
2	0	12	-	34.6	
3	0	12	-	61.2	
4	0	12	-	27.4	
1	0	-13	66.7	77.3	
2	0	-13	-	20.6	
3	0	-13	-	44.8	
4	0	-13	-	42.5	
5	0	-13	-	77.6	
6	0	-13	-	39.8	
7	0	-13	-	38.9	
8	0	-13	-	34.6	
9	0	-13	71.6	89.5	
10	0	-13	-	33.0	
11	0	-13	-	43.7	
12	0	-13	-	38.1	
13	0	-13	-	59.6	
0	0	13	-	23.1	
1	0	13	-	72.6	
0	1	0	-	57.3	
1	1	0	-	24.9	
2	1	0	26.5	26.2	
3	1	0	87.4	145.2	
4	1	0	44.3	40.8	
5	1	0	50.1	51.0	
6	1	0	48.3	45.5	
7	1	0	97.2	136.4	
8	1	0	27.8	24.3	
9	1	0	82.6	78.2	
10	1	0	-	11.8	
11	1	0	46.2	37.5	
12	1	0	67.3	66.9	
13	1	0	61.6	52.8	
14	1	0	41.4	37.0	
15	1	0	-	26.4	
16	1	0	44.6	42.0	
17	1	0	41.2	40.1	
18	1	0	41.1	57.9	
19	1	0	44.3	52.9	
1	1	-1	-	43.5	
2	1	-1	94.3	126.1	*
3	1	-1	100.4	127.0	*
4	1	-1	51.1	66.4	
5	1	-1	-	3.5	
6	1	-1	66.9	103.6	
7	1	-1	43.4	46.7	
8	1	-1	76.5	84.6	
9	1	-1	-	12.5	
10	1	-1	70.5	79.9	
11	1	-1	41.0	31.4	
12	1	-1	-	90.3	
13	1	-1	-	57.5	
14	1	-1	-	43.9	
15	1	-1	-	32.4	
16	1	-1	-	59.4	
17	1	-1	-	84.9	
18	1	-1	-	28.4	
19	1	-1	-	44.6	
0	1	1	-	36.7	
1	1	1	95.2	129.7	*
2	1	1	95.3	126.6	*
3	1	1	52.1	68.7	
4	1	1	-	7.0	
5	1	1	75.5	118.0	
6	1	1	51.5	65.7	
7	1	1	47.5	41.5	
8	1	1	33.6	38.3	
9	1	1	75.1	90.3	
10	1	1	43.9	33.1	
11	1	1	-	38.2	
12	1	1	-	66.2	
13	1	1	-	72.0	
14	1	1	-	12.5	
15	1	1	-	36.8	
16	1	1	-	55.6	
17	1	1	-	15.5	
18	1	1	-	49.7	
1	1	-2	80.7	89.1	
2	1	-2	107.2	137.5	*
3	1	-2	96.7	117.7	
4	1	-2	69.8	67.6	
5	1	-2	36.2	30.6	
6	1	-2	98.0	116.4	
7	1	-2	59.9	49.4	
8	1	-2	42.8	35.9	
9	1	-2	49.5	37.6	
10	1	-2	101.6	95.7	
11	1	-2	41.1	35.5	
12	1	-2	48.9	34.5	
13	1	-2	56.9	43.5	
14	1	-2	73.5	60.4	
15	1	-2	57.5	58.7	
16	1	-2	-	20.2	
17	1	-2	54.9	50.8	
18	1	-2	-	36.4	
19	1	-2	-	56.7	
0	1	2	108.6	179.6	*
1	1	2	97.2	119.9	
2	1	2	69.3	72.7	
3	1	2	54.0	53.4	
4	1	2	72.1	83.4	
5	1	2	55.5	53.6	
6	1	2	43.6	38.3	
7	1	2	55.3	50.0	
8	1	2	60.4	51.3	
9	1	2	52.8	44.6	
10	1	2	-	18.3	
11	1	2	95.4	98.2	
12	1	2	-	24.0	
13	1	2	62.8	65.1	
14	1	2	-	34.3	
15	1	2	77.5	94.8	
16	1	2	-	33.4	
17	1	2	-	68.9	
1	1	-3	74.9	73.7	
2	1	-3	64.0	62.5	
3	1	-3	31.9	25.5	
4	1	-3	54.0	50.1	
5	1	-3	80.8	83.7	
6	1	-3	91.5	89.2	
7	1	-3	46.1	42.9	
8	1	-3	-	18.1	
9	1	-3	106.0	101.6	
10	1	-3	94.3	82.7	
11	1	-3	43.4	37.4	
12	1	-3	46.1	44.1	
13	1	-3	73.1	74.7	
14	1	-3	64.5	52.6	
15	1	-3	57.1	49.8	
16	1	-3	-	53.4	
17	1	-3	-	30.8	
18	1	-3	-	43.9	
19	1	-3	-	37.2	
0	1	3	20.8	16.0	
1	1	3	21.9	17.8	
2	1	3	83.9	95.0	
3	1	3	93.8	102.9	
4	1	3	49.2	46.9	
5	1	3	35.0	29.0	
6	1	3	110.4	132.2	
7	1	3	102.9	94.9	
8	1	3	40.8	36.9	
9	1	3	53.1	41.8	
10	1	3	79.5	78.2	
11	1	3	-	30.1	
12	1	3	-	30.3	
13	1	3	-	13.2	
14	1	3	-	25.0	
15	1	3	-	34.7	
16	1	3	-	19.1	
17	1	3	-	10.6	
1	1	-4	72.7	62.9	
2	1	-4	53.3	42.5	
3	1	-4	72.9	76.6	
4	1	-4	103.4	120.7	
5	1	-4	77.2	77.1	
6	1	-4	44.8	43.9	
7	1	-4	83.7	87.1	
8	1	-4	77.8	64.1	
9	1	-4	91.0	77.3	
10	1	-4	-	15.5	
11	1	-4	58.8	40.6	
12	1	-4	-	16.0	
13	1	-4	49.0	35.3	
14	1	-4	73.2	80.1	
15	1	-4	-	29.7	
16	1	-4	53.1	44.5	
17	1	-4	-	12.1	
18	1	-4	78.5	104.7	
19	1	-4	-	21.9	
0	1	4	100.3	122.1	
1	1	4	56.2	58.8	
2	1	4	41.7	33.3	
3	1	4	76.4	69.4	
4	1	4	63.6	54.7	
5	1	4	39.6	36.8	
6	1	4	-	30.3	
7	1	4	61.8	45.8	
8	1	4	61.7	53.9	
9	1	4	46.1	39.2	
10	1	4	68.6	75.6	
11	1	4	50.8	37.4	
12	1	4	69.9	68.5	
13	1	4	-	29.4	
14	1	4	58.6	70.7	
15	1	4	62.1	59.9	
16	1	4	-	58.6	
1	1	-5	90.8	99.9	
2	1	-5	65.9	57.7	
3	1	-5	66.0	68.0	
4	1	-5	66.9	58.7	
5	1	-5	36.7	30.8	
6	1	-5	-	6.4	
7	1	-5	79.6	63.8	
8	1	-5	108.7	100.5	
9	1	-5	66.6	56.7	
10	1	-5	-	10.3	
11	1	-5	57.2	45.0	
12	1	-5	116.4	116.7	
13	1	-5	52.6	46.3	
14	1	-5	-	6.1	
15	1	-5	-	25.3	
16	1	-5	75.3	78.4	
17	1	-5	-	11.2	
18	1	-5	-	32.4	
19	1	-5	-	11.3	
0	1	5	63.2	65.4	
1	1	5	47.1	43.2	
2	1	5	65.6	52.4	
3	1	5	105.1	120.2	
4	1	5	60.2	44.3	
5	1	5	-	16.5	
6	1	5	-	27.7	
7	1	5	83.1	81.7	
8	1	5	49.3	41.9	
9	1	5	-	19.8	
10	1	5	57.1	46.4	
11	1	5	59.2	48.1	
12	1	5	-	59.4	
13	1	5	-	14.4	
14	1	5	-	63.6	
15	1	5	-	16.8	
1	1	-6	70.8	59.0	
2	1	-6	58.8	52.0	
3	1	-6	108.6	102.6	
4	1	-6	51.5	41.4	
5	1	-6	81.0	79.4	
6	1	-6	70.3	62.8	
7	1	-6	107.7	98.0	
8	1	-6	67.8	48.1	
9	1	-6	49.5	40.7	
10	1	-6	59.7	51.7	
11	1	-6	51.9	44.5	
12	1	-6	65.2	54.2	
13	1	-6	72.2	57.6	
14	1	-6	56.1	44.0	
15	1	-6	-	32.0	
16	1	-6	-	34.3	
17	1	-6	72.7	83.5	
18	1	-6	-	40.5	
19	1	-6	-	28.7	
0	1	6	41.0	32.9	
1	1	6	83.2	67.0	
2	1	6	86.2	85.3	
3	1	6	44.8	43.1	
4	1	6	41.8	32.3	
5	1	6	-	28.0	
6	1	6	102.1	109.4	
7	1	6	-	33.8	
8	1	6	60.9	46.7	
9	1	6	54.6	46.0	
10	1	6	70.6	84.0	
11	1	6	-	20.1	
12	1	6	58.6	56.0	
13	1	6	-	18.1	
14	1	6	-	26.5	
1	1	-7	88.0	83.3	
2	1	-7	84.6	79.4	
3	1	-7	-	28.5	
4	1	-7	65.3	52.4	
5	1	-7	99.2	89.7	
6	1	-7	77.4	70.2	
7	1	-7	-	14.5	
8	1	-7	-	17.0	
9	1	-7	72.5	61.4	
10	1	-7	49.6	40.3	
11	1	-7	65.0	59.2	
12	1	-7	58.5	49.3	
13	1	-7	-	33.3	
14	1	-7	-	10.0	
15	1	-7	74.8	88.7	
16	1	-7	66.5	58.5	
17	1	-7	-	22.7	
18	1	-7	-	25.7	
19	1	-7	-	87.6	
0	1	7	60.2	48.5	
1	1	7	-	12.2	
2	1	7	79.9	73.1	
3	1	7	58.1	57.2	
4	1	7	57.9	50.2	
5	1	7	47.3	40.5	
6	1	7	69.4	60.5	
7	1	7	-	6.4	
8	1	7	52.5	45.6	
9	1	7	66.1	70.2	
10	1	7	-	15.0	
11	1	7	55.6	42.4	
12	1	7	-	51.8	
1	1	-8	43.3	42.1	
2	1	-8	-	16.3	
3	1	-8	56.1	45.2	
4	1	-8	51.8	42.5	
5	1	-8	56.2	46.7	
6	1	-8	45.3	45.5	
7	1	-8	-	9.3	
8	1	-8	-	22.4	
9	1	-8	111.5	118.2	
10	1	-8	-	40.9	
11	1	-8	-	40.5	
12	1	-8	-	34.9	
13	1	-8	102.3	104.0	
14	1	-8	-	6.4	
15	1	-8	-	42.3	

Table 2. Continued.

h	k	l	$\lvert F_o \rvert$	$\lvert F_c \rvert$	h	k	l	$\lvert F_o \rvert$	$\lvert F_c \rvert$	h	k	l	$\lvert F_o \rvert$	$\lvert F_c \rvert$	h	k	l	$\lvert F_o \rvert$	$\lvert F_c \rvert$	h	k	l	$\lvert F_o \rvert$	$\lvert F_c \rvert$
16	1	-8	-	18.2	8	1	-9	62.4	59.1	2	1	-10	50.3	50.1	7	1	10	-	65.4	4	1	11	-	59.0
17	1	-8	-	26.0	9	1	-9	77.5	70.5	3	1	-10	90.0	91.4	8	1	10	-	74.1	5	1	11	-	20.3
18	1	-8	-	29.9	10	1	-9	-	28.5	4	1	-10	-	19.8	1	1	-11	-	14.0	6	1	11	-	65.0
19	1	-8	-	12.8	11	1	-9	-	17.0	5	1	-10	49.6	42.1	2	1	-11	-	32.6	1	1	-12	62.0	75.5
0	1	8	-	18.8	12	1	-9	-	28.6	6	1	-10	95.6	90.4	3	1	-11	53.1	68.9	2	1	-12	-	40.7
1	1	8	84.5	88.5	13	1	-9	59.1	59.9	7	1	-10	63.0	78.3	4	1	-11	-	28.4	3	1	-12	-	31.9
2	1	8	40.4	43.7	14	1	-9	60.3	48.0	8	1	-10	58.5	58.1	5	1	-11	-	25.3	4	1	-12	-	45.1
3	1	8	79.2	88.1	15	1	-9	-	38.3	9	1	-10	-	27.4	6	1	-11	-	30.5	5	1	-12	-	31.4
4	1	8	-	9.1	16	1	-9	-	6.1	10	1	-10	-	26.0	7	1	-11	55.9	46.5	6	1	-12	67.2	83.8
5	1	8	-	34.1	17	1	-9	-	69.0	11	1	-10	58.9	59.1	8	1	-11	-	26.2	7	1	-12	-	17.3
6	1	8	58.4	63.3	18	1	-9	-	66.7	12	1	-10	-	28.9	9	1	-11	59.9	58.6	8	1	-12	61.6	60.8
7	1	8	73.2	66.9	0	1	9	89.9	93.8	13	1	-10	-	39.9	10	1	-11	43.2	57.3	9	1	-12	-	22.9
8	1	8	-	23.1	1	1	9	-	27.2	14	1	-10	-	21.0	11	1	-11	-	11.4	10	1	-12	67.8	76.6
9	1	8	-	11.8	2	1	9	-	36.3	15	1	-10	-	19.3	12	1	-11	41.5	47.7	11	1	-12	-	14.5
10	1	8	-	51.4	3	1	9	-	32.8	16	1	-10	-	28.0	13	1	-11	-	46.7	12	1	-12	-	38.8
11	1	8	-	31.9	4	1	9	58.6	58.4	17	1	-10	-	49.2	14	1	-11	-	14.9	13	1	-12	-	24.4
1	1	-9	62.5	52.9	5	1	9	65.6	65.4	0	1	10	-	15.5	15	1	-11	-	37.0	14	1	-12	-	66.1
2	1	-9	95.5	75.7	6	1	9	-	46.2	1	1	10	92.4	56.0	16	1	-11	-	24.6	15	1	-12	-	27.5
3	1	-9	-	10.3	7	1	9	-	18.4	2	1	10	-	38.5	17	1	-11	-	28.5	0	1	12	-	15.0
4	1	-9	93.7	94.3	8	1	9	-	32.6	3	1	10	-	39.3	0	1	11	63.5	74.0	1	1	12	-	38.1
5	1	-9	53.0	54.9	9	1	9	-	68.5	4	1	10	-	21.8	1	1	11	-	66.1	2	1	12	-	19.1
6	1	-9	43.3	42.2	10	1	9	-	37.1	5	1	10	-	41.9	2	1	11	-	60.3	3	1	12	-	86.6
7	1	-9	-	18.4	1	1	-10	-	19.9	6	1	10	-	36.2	3	1	11	-	15.8	4	1	12	-	31.6

also 1.2 but with an individual spread within usual estimation errors ($\pm$ 20 %). This value was used to calculate the contributions from the different individuals to the overlapped reflexions along the a^*-axis. In the Mo-material most of the reflexions along the first festoons on both sides of the a^*-axis are completely overlapped. These reflexions do not have the same indices from the two individuals and, consequently, they cannot be separated by means of the volume fraction only. They were instead separated by making use of the values from the Cu-material.

From the material separated in this way, the values from the larger individual were first used for the further calculations.

The same least-squares program was used as before and the same parameters were varied, whilst 458 $h0l$ and $h1l$ reflexions were used. Before the last cycles of the refinement, the 14 reflexions with the strongest intensities were omitted

Table 3. Final structure data for Mo_8P_5. Standard deviations for the parameters are given in parentheses.

Space group: Pm; $Z = 1$
$a = 9.3992(9)$ Å; $b = 3.2088(4)$ Å; $c = 6.5369(7)$ Å;
$\beta = 109.592(8)°$; $U = 185.7$ Å^3

Atom	Position	x	z	B(Å^2)
Mo(1)	1(*a*)	0[a]	0[a]	−0.54(7)
Mo(2)	1(*a*)	0.7806(9)	0.2390(13)	−0.33(8)
Mo(3)	1(*a*)	0.2468(9)	0.7931(13)	−0.40(8)
Mo(4)	1(*a*)	0.3061(9)	0.3569(13)	−0.42(8)
Mo(5)	1(*a*)	0.5706(9)	0.7939(13)	−0.52(8)
Mo(6)	1(*b*)	0.0529(9)	0.3937(13)	−0.12(9)
Mo(7)	1(*b*)	0.7805(8)	0.6113(13)	−0.53(7)
Mo(8)	1(*b*)	0.4977(8)	0.1232(13)	−0.39(8)
P(1)	1(*a*)	0.5831(24)	0.4301(35)	−0.10(28)
P(2)	1(*a*)	0.9856(22)	0.6236(34)	−0.27(25)
P(3)	1(*b*)	0.2090(23)	0.0659(34)	−0.20(25)
P(4)	1(*b*)	0.3716(23)	0.6553(33)	−0.19(25)
P(5)	1(*b*)	0.7858(25)	0.9813(35)	−0.21(26)

Final R-value = 0.119

[a] Arbitrarily.

in order to reduce extinction effects. The final shifts of the parameters were less than 1 % of the standard deviations. The standard deviations are somewhat larger than is usual in contemporary structure determinations from this institute. This may be due to deficiencies in the material because of the twinning and the presence of the "extra" satellites.

A difference synthesis calculated after the refinement showed no abnormal features. The largest positive and negative parts of the difference map were less than 20 % of the phosphorus peaks in the $\varrho_o(xz)$ synthesis.

Observed and calculated structure factors are listed in Table 2. Final structural data are given in Table 3. In this case probably no regard should be paid to the temperature factors. The extreme values may be caused by the abnormal absorption conditions which arise because of the presence of a twin individual (or perhaps several parallelly oriented ones), which in different positions "hides" the first individual (one or more) to a varying degree.

The results from the Cu-data are in rather good accordance with those from the Mo-data, considering the greater errors in the Cu-data.

*Control refinements (*Mo-*material).* A refinement of the material from the smaller twin individual gave results in agreement with those obtained from the larger one. Thus, the deviations for all the parameters are less than three standard deviations. All the temperature factors, except for one phosphorus atom, were negative.

As mentioned above, it is possible to work in a somewhat different way with twin material of this sort. Here use is made of the fact that reflexions of the types $h0l$ and $h+l$, $0,-l$ (for this case) are related by the (100) plane. The corresponding relation is valid for the hll layer. These reflexions are called "related reflexions". The intensities for the overlapped reflexions are corrected to a "sum crystal" oriented as the larger of the individuals. Use is then made of the formula

$$I_c = I_o + \alpha(I_o - I_o') \tag{1}$$

where I_c = corrected intensity, I_o = observed intensity for a reflexion, I_o' = observed intensity for the related reflexion, $\alpha = f/(1-2f)$, where f is the "twin fraction" (*i.e.* the ratio of the volume of the smaller component to the total volume). The method is described in detail by Grainger,[18] and relation (1) is also given by Zachariasen and Plettinger.[19]

In the present case the two components are of about the same size

$$\left.\begin{matrix}\text{Mean value}\\ \text{of the ratio}\end{matrix}\right\} \frac{I(hkl)_2}{I(hkl)_1} = \frac{\text{volume of "2"}}{\text{volume of "1"}} = \frac{1-f}{f} = 1.2$$

which gives $f = 0.45$ and $\alpha = 4.5$. As Grainger pointed out the correction would fail when both crystals have the same volume ($f = 0.5$). The "related reflexions" would then be of equal intensity and α would be infinite. In the present case the difference $I_o - I_o'$ will be small and sensitive to errors in the estimation of intensities, and thus when this term is multiplied with the large value of α the term $\alpha(I_o - I_o')$ will be rather uncertain. The method is therefore probably most suitable when working with diffraction data from a large crystal with a smaller crystallite in twin orientation.

Two refinements were made on the data from the "sum crystal". In the first, only separated reflexions were used and for these the intensities from reflexions with the same index from the two individuals were added. In the second refinement even overlapped reflexions (treated as decribed above) were included. However, the number of overlapped reflexions is rather small. The results of these refinements are in agreement with those for the individuals. The deviations of the parameters are less than three standard deviations. The temperature factors are negative and the R-values about the same as for the other refinements (~ 0.12).

DESCRIPTION AND DISCUSSION OF THE Mo_8P_5 STRUCTURE

Untwinned structure. A projection of the structure along the monoclinic axis is illustrated in Fig. 5. The notations in the figure correspond to those used for the different crystallographic positions in Tables 3 and 4.

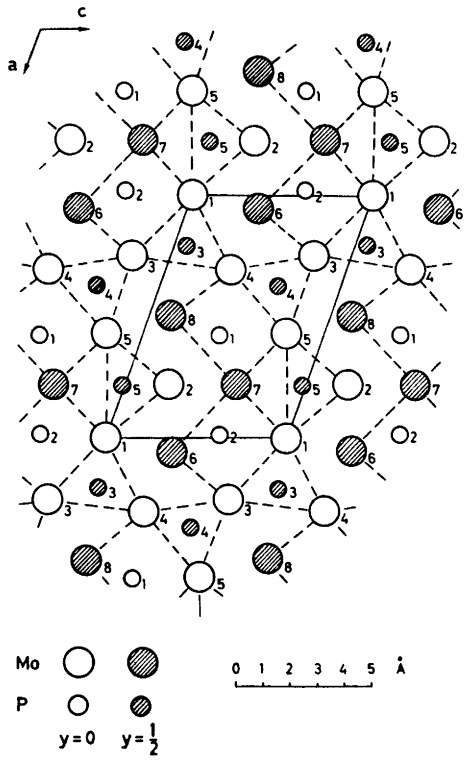

Fig. 5. The crystal structure of Mo_8P_5 projected on (010). The PMo_6 triangular prisms are indicated by broken lines, these lines are only for the purpose of emphasizing special features of the structure.

Some of the characteristic features of the structure can be mentioned. As pointed out above, the atoms in the unit cell are situated in two layers, separated by $b/2$. The b-axis is short, being only 3.209 Å, this value also corresponds to the shortest P – P distance. The immediate environment of the phosphorus atoms, accordingly, consists of molybdenum atoms only. All the phosphorus atoms have a triangular prismatic environment with 1 – 3 additional metal atoms situated outside the quadrilateral faces of the more or less distorted prisms. The triangular faces of the P(1) and P(2) prisms are perpendicular to (010), while the triangular faces of the P(3), P(4), and P(5) prisms are parallel to this plane. The features mentioned are characteristic for metal-rich phosphides of transition metals (and also for arsenides, sulphides and selenides). The structures can be described as arrays of interconnected PMe_6-prisms, the prisms being packed in relation to each other (and in some cases with other coordination figures), in different ways to give a rather dense

Table 4. Interatomic distances in Mo_8P_5 (in Ångström units). Only distances shorter than 3.8 Å are listed. Standard deviations are given in parentheses.

Mo(1) –	P(2)	2.418(21)	Mo(6) –	P(3)	2.976(22)
– 2	P(3)	2.460(15)	–	P(5)	3.005(23)
– 2	P(5)	2.545(17)	– 2	Mo(3)	3.086(10)
– 2	Mo(6)	2.930(7)	– 2	Mo(6)	3.209(0)
–	Mo(2)	2.975(8)	–	Mo(7)	3.319(11)
–	Mo(4)	3.036(8)			
–	Mo(3)	3.052(8)	Mo(7) –	P(5)	2.402(23)
– 2	Mo(7)	3.126(7)	– 2	P(1)	2.439(17)
– 2	Mo(1)	3.209(0)	– 2	P(2)	2.488(16)
			– 2	Mo(2)	2.915(9)
Mo(2) – 2	P(5)	2.339(17)	– 2	Mo(5)	3.078(9)
–	P(1)	2.562(23)	– 2	Mo(1)	3.126(7)
–	P(2)	2.605(22)	– 2	Mo(7)	3.209(0)
– 2	Mo(6)	2.900(10)	–	Mo(6)	3.319(11)
– 2	Mo(7)	2.915(9)	–	Mo(8)	3.400(11)
–	Mo(5)	2.917(11)			
–	Mo(1)	2.975(8)	Mo(8) – 2	P(1)	2.482(17)
– 2	Mo(8)	2.978(9)	–	P(3)	2.612(22)
– 2	Mo(2)	3.209(0)	–	P(4)	2.886(22)
			– 2	Mo(5)	2.944(10)
Mo(3) –	P(2)	2.331(21)	– 2	Mo(2)	2.978(9)
– 2	P(4)	2.339(16)	– 2	Mo(3)	3.063(9)
– 2	P(3)	2.511(17)	–	P(5)	3.143(23)
–	Mo(5)	3.041(11)	– 2	Mo(4)	3.162(10)
–	Mo(1)	3.052(8)	– 2	Mo(8)	3.209(0)
– 2	Mo(8)	3.063(9)	–	Mo(7)	3.400(11)
–	Mo(4)	3.083(11)			
– 2	Mo(6)	3.086(10)	P(1) –	Mo(5)	2.420(23)
– 2	Mo(3)	3.209(0)	– 2	Mo(7)	2.439(17)
–	Mo(4)	3.538(11)	– 2	Mo(8)	2.482(17)
			–	Mo(4)	2.484(23)
Mo(4) – 2	P(3)	2.421(17)	–	Mo(2)	2.562(23)
– 2	P(4)	2.440(17)	– 2	P(1)	3.209(0)
–	P(1)	2.484(23)	– 2	P(4)	3.264(26)
– 2	Mo(6)	2.946(10)	–	P(2)	3.564(29)
–	Mo(1)	3.036(8)			
–	Mo(3)	3.083(11)	P(2) –	Mo(3)	2.331(21)
–	Mo(5)	3.095(11)	–	Mo(1)	2.418(21)
– 2	Mo(8)	3.162(10)	– 2	Mo(6)	2.423(17)
– 2	Mo(4)	3.209(0)	– 2	Mo(7)	2.488(16)
–	Mo(3)	3.538(11)	–	Mo(2)	2.605(22)
			– 2	P(2)	3.209(0)
Mo(5) – 2	P(4)	2.399(16)	– 2	P(3)	3.357(26)
–	P(1)	2.420(23)	–	P(1)	3.564(29)
– 2	P(5)	2.551(18)			
–	Mo(2)	2.917(11)	P(3) – 2	Mo(4)	2.421(17)
– 2	Mo(8)	2.944(10)	– 2	Mo(1)	2.460(15)
–	Mo(3)	3.041(11)	– 2	Mo(3)	2.511(17)
– 2	Mo(7)	3.078(9)	–	Mo(8)	2.612(22)
–	Mo(4)	3.095(11)	–	Mo(6)	2.976(22)
– 2	Mo(5)	3.209(0)	– 2	P(3)	3.209(0)
			– 2	P(2)	3.357(26)
Mo(6) – 2	P(2)	2.423(17)	–	P(4)	3.506(29)
– 2	Mo(2)	2.900(10)	–	P(4)	3.638(29)
–	P(4)	2.909(22)			
– 2	Mo(1)	2.930(7)			
– 2	Mo(4)	2.946(10)			

Table 4. Continued.

P(4)	−2	Mo(3)	2.339(16)	P(5)	−	Mo(6)	3.005(23)
	−2	Mo(5)	2.399(16)		−	Mo(8)	3.143(23)
	−2	Mo(4)	2.440(17)		−2	P(5)	3.209(0)
	−	Mo(8)	2.886(22)		−	P(4)	3.760(30)
	−	Mo(6)	2.909(22)				
	−2	P(4)	3.209(0)				
	−2	P(1)	3.264(26)				
	−	P(3)	3.506(29)				
	−	P(3)	3.638(29)				
	−	P(5)	3.760(30)				
P(5)	−2	Mo(2)	2.339(17)				
	−	Mo(7)	2.402(23)				
	−2	Mo(1)	2.545(17)				
	−2	Mo(5)	2.551(18)				

packing of the metal atoms. Mo_8P_5 is a new structure type with a new kind of packing of the prism structure elements. Several other ways of packing the prisms have been found in structures which have been determined at this Institute in recent years, for instance: Mo_4P_3,[4] Ta_2P,[20] Nb_7P_4,[2] Hf_3P_2,[21] Nb_5P_3,[22] and Nb_4As_3.[23] The characteristic features are discussed more in the detail in articles by Rundqvist [24] and Lundström,[7] where several other examples can be found.

Interatomic distances are to be found in Table 4.

Comparing the Mo − P distances with the sum of the Goldschmidt 12-coordination radius for molybdenum, 1.40 Å, and the tetrahedral covalent radius for phosphorus, 1.10 Å, it can be seen that some Mo − P distances are somewhat short, the shortest being only 2.33 Å. However, considering the standard deviations and comparing with other similar structures (for instance Mo_4P_3,[4] with distances down to 2.35 Å), the distances obtained are certainly reasonable.

Moreover it can be mentioned that the different P − Mo distances are in good agreement with general observations (given in Ref. 24), concerning phosphorus-metal distances in this class of structure.

The Mo − Mo interatomic distances are also largely in good accordance with the size-factor principle given in the latter reference. As in similar structures the coordination numbers around the molybdenum atoms are rather high, 14 − 15 and perhaps even 16.

Structure of twin interface. Twinning can be discussed from several points of view. One is to consider the geometrical (symmetry) aspects of the *lattice* (and the structure in relation to this). Observations of twinning relationships can then be systematized by what may be called "the empirical rules of twinning of the French School", which have been summarized by Friedel,[25] and explained in English by Cahn.[11] Apart from this approach, it is also important to consider the structure itself, as was pointed out by Buerger,[26] and discussed by Cahn.[11] Buerger makes the point (p. 475) that the rules of the French theory "provide, perhaps, necessary conditions for certain twins to occur, but they are definitely not sufficient conditions". An important factor is consequently the degree of structural disturbance at the twin

boundaries. Quoting Cahn (p. 379), it can be said: " One would expect the state of disturbance of the crystal structure at the interface between the components to be particularly slight in the substances in which twins can in fact be obtained."

As an extra note on the geometrical features in addition to those given in previous sections, it can be noted that the obliquity angle (19.6°) for the pseudo-merohedral type of twinning observed in the present investigation is unusually large. However, it is possible to choose a larger *B*-centred unit cell ($a = 17.7116(17)$ Å; $b = 3.2088(4)$ Å; $c = 6.5369(7)$ Å; $\beta = 89.245(8)°$; $U = 371.5$ Å^3), with a much smaller twin obliquity (about 0.8°). This cell is probably the more desirable in considering the pseudo-symmetry.

The structural fit between the twinned individuals in the vicinity of the common plane (*i.e.* the twin plane, if there is one) can be studied in terms of the structural consequences of the different twin laws. As mentioned above, one obtains different atomic arrangements for the different possible twin operations. The choice of the unit cell is arbitrary in Fig. 5, and the origin (or the common plane) can be chosen in another more appropriate way. Some conceivable possibilities giving minimal disturbance at the interface are discussed here. Although no *a priori* assumption can be made that the common plane is the interface between the individuals, and although no study of this interface was made in the present investigation, it is assumed in the figures that the former is the case. The twins would then be contact twins [11] (possibly lamellar twins [11]). If the twin plane is also the twin boundary the distortion is small, but as the overlapping of the atomic positions from the respective individuals in the area of the boundary is good, some penetration may be possible (penetration twins [11]).

One of the possible twin operations for type A was a 180° rotation about the normal to the (100) plane. By choosing the unit cell (or strictly speaking the (100) plane) as in Fig. 6 one can obtain an interface in which the disturbance is rather slight. It can be seen that the same types of coordination figures exist in the immediate vicinity of the interface as in the main structure, even if they are here somewhat differently distorted. At the interface P(1) "co-ordinates" Mo(3) instead of Mo(4). Accordingly Mo(4) will have only four phosphorus neighbours, while Mo(3) has six; P(1), however, being so distant that it can hardly be considered as a neighbour. The interatomic distance Mo(4)–Mo(5) or Mo(4)–Mo(8) (the choice depending on the displacement along the (100) plane) will be somewhat shorter than metal–metal distances in the main structure, although small adjustments of the atomic positions are quite conceivable. That a proposal of this general type ought to give a reasonable result can be inferred from the structure (Fig. 5) considering that the atoms are situated approximately in "planes" parallel to the (100) plane.

A better proposal can be obtained through the other possible twin operation for type A. This operation was a 180° rotation about the *c*-axis. From a structural point of view, this is, for the present structure, equivalent with a reflexion across the (100) plane. The unit cell is chosen so that the (100) plane is in the vicinity of Mo(2), for instance in such a way that the *c*-axis passes exactly through this atom. Mo(7) and P(5) will then almost lie in the (100) plane. From Fig. 5 it can be seen that *the structure itself* has a "pseudo-mirror

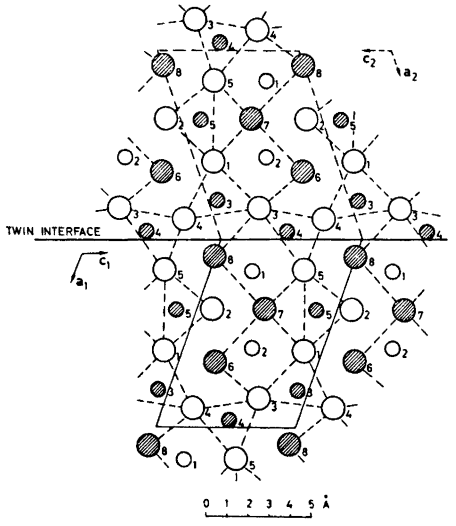

Fig. 6. Proposal for twin arrangement (orientation: type A, alt. 1). Notations and projection as in Fig. 5.

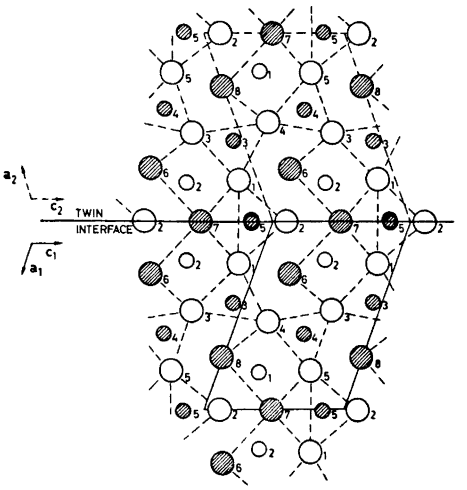

Fig. 7. Proposal for twin arrangement (orientation: type A, alt. 2).

plane" here. Fig. 7 shows one of the possibilities for the twins in this arrangement. Small movements in the area of the twin interface are necessary for Mo(7) and specially for P(5), which has to be moved to the interface. (Alternatively one of the double atomic sites in the figure can be left vacant.) The coordination figures are similar to those in the main structure. All the interatomic distances will be normal. Thus, this arrangement appears to be very plausible and it is perhaps the most probable one for type A.

For the second "twin type" (B) the planes $(\bar{1}01)_1$ and $(001)_2$, from the two individuals, respectively, constitute the common plane. Depending on the direction of the *a*-axis of the second individual two different arrangements can be obtained. In Fig. 8 one possible example of this kind is shown. The second individual (to the right) is rotated, in relation to the first by 40.5° around the common *b*-axis (there will be complete coincidence of the *b*-axes just below the picture) or the second individual is first rotated 180° about the normal to the (100) plane and then 180° about its own *a*-axis (small adjustments of the atomic positions are necessary, *cf.* Fig. 4). Some small atomic displacements may also be necessary depending on the fact that the length of the face diagonal (9.480 Å) is not exactly the same as that of the *a*-axis (9.399 Å). For instance, Mo(6) and Mo(8) can be made to overlap completely by such small displacements. For the sake of clearness several unit cells for the orientations of both individuals are drawn. Also in this case the usual sorts of coordination figures are preserved at the twin interface, even if they are somewhat distorted. P(4) and Mo(2) must be moved somewhat away from each other. Alternatively, it is possible to imagine some penetration into the left individual in this area.

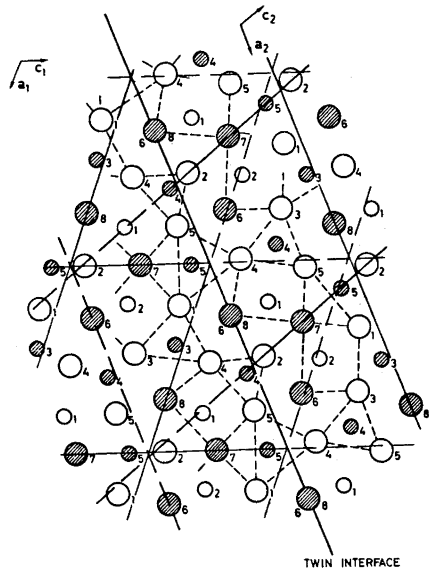

Fig. 8. Proposal for twin arrangement (orientation: type B, alt. 1).

Directly arising from the structure itself (Fig. 5) a conceivable explanation of twin orientation according to this proposal can be seen. The somewhat remarkable environment around Mo(8) is rather similar to that around Mo(6), but the surroundings are rotated (about 40°) with respect to each other. (The metal environment around these atoms can be regarded as very distorted cubic. The "cube" around Mo(8), for instance, is composed of the molybdenum atoms designated 2, 5, 3, and 4. Moreover there is an additional metal atom, Mo(7), outside the large "cube face" and five phosphorus "neighbours". The large "cube faces", Mo(4), (4), (2), (2), and Mo(2), (2), (3), (3), respectively, would then be roughly parallel to the planes (001) and ($\bar{1}$01), respectively.)

The special structural features of Mo_8P_5 discussed here give the structure the special property of being able to continue itself in an alternative twin configuration (two different orientations) without involving a large violation of the geometrical requirements of its atoms in the nearest coordination shells. The boundary then has a low energy whereby the twin is energetically possible.[26] This is perhaps the reason for the very large frequency of twins, which has been observed in the crystalline material studied in this investigation.

Acknowledgements. I wish to thank Professors G. Hägg and I. Olovsson for all the facilities placed at my disposal. For my introduction to this interesting field of research I am indebted to Professor S. Rundqvist and Dr. I. Engström. I also wish to thank Prof. Rundqvist for valuable advice, stimulating discussions and his interest in this work. I am indebted to Dr. M. Richardson for the revision of the English text.

The work has been supported financially by the *Swedish Natural Science Research Council.*

REFERENCES

1. Rundqvist, S. *Nature* **211** (1966) 847.
2. Rundqvist, S. *Acta Chem. Scand.* **20** (1966) 2427.
3. Sellberg, B. and Rundqvist, S. *Acta Chem. Scand.* **19** (1965) 760.
4. Rundqvist, S. *Acta Chem. Scand.* **19** (1965) 393.
5. Rundqvist, S. and Lundström, T. *Acta Chem. Scand.* **17** (1963) 37.
6. Rundqvist, S. and Nawapong, P. C., University of Uppsala. *Private communication*, 1966.
7. Lundström, T. *Arkiv Kemi* **31** (1969) 227.
8. *International Tables for X-Ray Crystallography*, Kynoch Press, Birmingham 1962, Vol. III.
9. Cruickshank, D. W. J., Philling, D. E., Bujosa, A., Lovell, F. M. and Truter, M. R. *Computing Methods and the Phase Problem*, Pergamon, Oxford 1961, p. 32.
10. Donnay, J. D. H. and Donnay, G. *International Tables for X-Ray Crystallography*, Kynoch Press, Birmingham 1959, Vol. II, p. 104.
11. Cahn, R. W. *Advan. Phys.* **3** (1954) 363.
12. Herbstein, F. H. *Acta Cryst.* **17** (1964) 1094.
13. Herbstein, F. H. *Acta Cryst.* **18** (1965) 997.
14. Herbstein, F. H. *Acta Cryst.* **19** (1965) 590.
15. Grainger, C. T. and McConnell, J. F. *Acta Cryst.* **A 25** (1969) 422.
16. Grainger, C. T. and McConnell, J. F. *Acta Cryst.* **B 25** (1969) 1962.
17. Grainger, C. T. *Acta Cryst.* **A 25** (1969) 435.
18. Grainger, C. T. *Acta Cryst.* **A 25** (1969) 427.
19. Zachariasen, W. H. and Plettinger, H. A. *Acta Cryst.* **18** (1965) 710.
20. Nylund, A. *Acta Chem. Scand.* **20** (1966) 2393.
21. Lundström, T. *Acta Chem. Scand.* **22** (1968) 2191.
22. Hassler, E. *Acta Chem. Scand.* **25** (1971) 129.
23. Carlsson, B. and Rundqvist, S. *Acta Chem. Scand.* **25** (1971) 1742.
24. Rundqvist, S. *Arkiv Kemi* **20** (1962) 67.
25. Friedel, G. *Leçons de cristallographie*, Berger-Levrault, Paris 1926.
26. Buerger, M. J. *Am. Mineralogist* **30** (1945) 469.

Received May 3, 1971.